

Journal Pre-proof

Redox-active ferrocene-containing Iridium(III) complex for non-volatile flash memory

Baojie Yang, Yongjing Deng, Peng Tao, Menglong Zhao, Weiwei Zhao, Runze Tang, Chenxi Ma, Qi Tan, Shujuan Liu, Qiang Zhao



PII: S1566-1199(20)30201-9

DOI: <https://doi.org/10.1016/j.orgel.2020.105815>

Reference: ORGELE 105815

To appear in: *Organic Electronics*

Received Date: 25 February 2020

Revised Date: 26 April 2020

Accepted Date: 9 May 2020

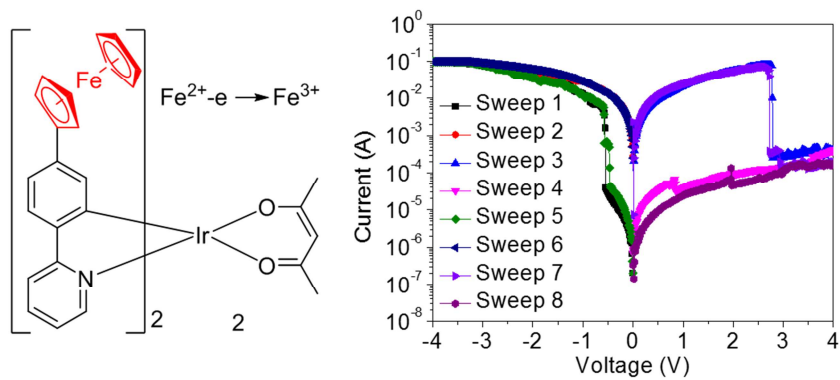
Please cite this article as: B. Yang, Y. Deng, P. Tao, M. Zhao, W. Zhao, R. Tang, C. Ma, Q. Tan, S. Liu, Q. Zhao, Redox-active ferrocene-containing Iridium(III) complex for non-volatile flash memory, *Organic Electronics* (2020), doi: <https://doi.org/10.1016/j.orgel.2020.105815>.

This is a PDF file of an article that has undergone enhancements after acceptance, such as the addition of a cover page and metadata, and formatting for readability, but it is not yet the definitive version of record. This version will undergo additional copyediting, typesetting and review before it is published in its final form, but we are providing this version to give early visibility of the article. Please note that, during the production process, errors may be discovered which could affect the content, and all legal disclaimers that apply to the journal pertain.

© 2020 Published by Elsevier B.V.

Graphical Abstract

Ferrocene-containing iridium(III) complex is rationally designed and synthesized for non-volatile flash memory induced by redox memory mechanism.



Title: Redox-Active Ferrocene-Containing Iridium(III) Complex for Non-Volatile Flash Memory

Authors: Baojie Yang, Yongjing Deng, Peng Tao, Menglong Zhao, Weiwei Zhao, Runze Tang, Chenxi Ma, Qi Tan, Shujuan Liu,* Qiang Zhao*

Address: Key Laboratory for Organic Electronics and Information Displays & Jiangsu Key Laboratory for Biosensors, Institute of Advanced Materials (IAM), Nanjing University of Posts and Telecommunications (NUPT), Nanjing 210023, P. R. China.

Corresponding E-mail: iamsjliu@njupt.edu.cn; iamqzhao@njupt.edu.cn

Keywords: iridium(III) complexes; ferrocene; memory devices; flash; redox

Abstract: A new ferrocene-containing iridium(III) complex (complex **2**) has been designed and synthesized. Its structure, photophysical property, electrochemistry and memory behaviors were well investigated. The memory device with a sandwich structure of ITO/complex **2**/Al (**D2**) exhibited flash memory performance with a bistable conductive process, which showed a high ON/OFF current ratio of 10^3 , long retention time of 10^3 s, and low threshold voltage of -0.55 V. After 10^5 read cycles, no significant degradation was observed in the ON and OFF states at a read voltage of 1.0 V. The ferrocene group of complex **2** serves as the redox-active unit, and a redox memory mechanism is proposed to explain the conductive process based on the analysis of I–V, cyclic voltammetry and theoretical calculation data. Thus, the design of redox-active metal complex used for novel non-volatile memory device provided an alternative strategy for the further development of organic memory materials and devices.

1. Introduction

The new-generation memory technology has been rapidly developed in the era of the information explosion.¹⁻⁴ However, downscaling of cell size and growing demand for memory materials of conventional memory devices based on inorganic semiconductors limit their further development in performance improvement and application expansion.^{5,6} Compared with traditional inorganic semiconductor devices, organic non-volatile memory has opened up a new way for the innovation of memory devices due to their promising merits of low manufacturing cost, three-dimensional stacking, large-scale thin-film formation, structural diversity and good scalability.⁵⁻¹⁰ Hence, organic materials have attracted increasing research interests and non-volatile organic memory devices have become a hot research area.¹¹⁻¹⁵ Organic non-volatile memory devices store information based on the bistability of materials, which can be encoded “0” and “1” as the charge stored in response to the high (ON) and low conductivity (OFF), respectively.¹⁶⁻¹⁹ Most recently, memory switching mechanisms can be proposed to filamentary conduction, space charge-limited current, redox switching, charge transfer, conformational changes, *etc.*²⁰⁻²⁷ Furthermore, various memory effects, such as flash,²⁸ resistive random access memory (RRAM), write-once read-many-times (WORM), static random access memory (SRAM) and dynamic random access memory (DRAM), have been recognized successfully.²⁹⁻³¹ However, there are few works on the preparation of small molecule-based flash memory devices. Therefore, there is an urgent to explore new organic flash memory materials and devices based on small molecules.

To date, small molecule based memory devices have aroused tremendous interest due to their attractive features such as easy fabrication, high flexibility, high purity, and synthetic versatility.^{32, 33} And in the meanwhile, a large number of ferrocene-containing materials have been synthesized and applied in biosensors, crystals, magnetic ceramics and organic cathode materials due to the outstanding features of ferrocene, such as 3D structure, thermal stability and redox activity.³⁴⁻³⁶ Although ferrocene (Fe^{2+}) and ferrocenium (Fe^{3+}) ions have excellent redox properties, few works have been reported on the memory properties of ferrocene-containing

small molecules. Chen. et al. reported an interesting memristive processing-memory. By introducing redox active moieties of triphenylamine and ferrocene, the polymer exhibits triple oxidation behavior and interesting memristive switching characteristics.³⁷ Guan and co-workers have reported that the conductive behavior of memory device can be enhanced based on ferrocene due to the redox responsiveness of ferrocene, in which Fe^{2+} can be oxidized to Fe^{3+} under an external electric field and the Fe^{3+} can return to Fe^{2+} when a reverse voltage is applied.³⁸ As a result, the stable redox properties of ferrocene-containing complexes provide the possibility of non-volatility and the stability of small molecule memory device.

Iridium(III) complexes have good chemical stability, thermal stability and rich charge-transfer excited state properties, which are very sensitive to the external stimuli and suitable for application in memory devices. Especially, the rich and strong charge transfer interaction between metal center and organic ligand can achieve electrical bistability through electric field induced charge transfer, resulting in a low threshold voltage.³⁹⁻⁴¹ Low power consumption memory requires low operating voltage. Chen. et al. found that the resultant pyrolytically modified product “pyro-MoS₂-PAN” shows good non-volatile rewritable memory performance after annealing at 220 °C for 4 h with a lower switching voltage of -1.09 V.²⁸ In this work, two kinds of iridium(III) complexes (complex **1** and **2**) were designed and synthesized to study the characteristics of electrical bistability for small-molecule non-volatile memory (**Figure 1**). The memory device with a sandwich structure of ITO/complex/aluminum (Al) were prepared respectively. Memory device based on complex **1** (**D1**) showed no memory characteristics, while complex **2**-based device exhibited typical flash characteristics. The memory behavior of complex **2** is induced by the introduction of ferrocene moiety into the C^N ligand. The ON/OFF current ratio of **D2** is as high as 10^3 with a low switched voltage of -0.55 V. It exhibits long retention time of 10^3 s. After 10^5 read cycles, no significant degradation was observed in the ON and OFF states at a read voltage of 1.0 V. A redox memory mechanism is proposed to explain the conductive process.

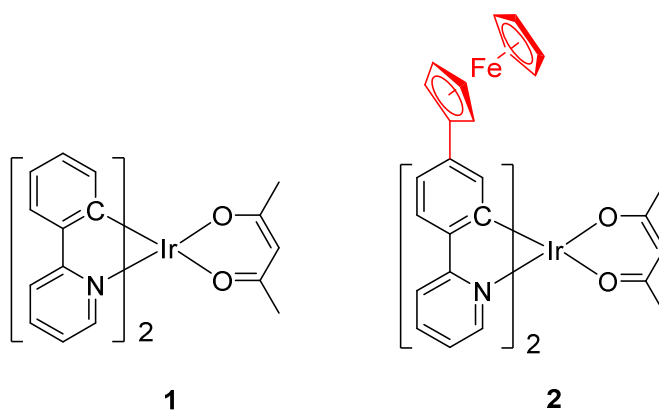


Figure 1. Chemical structures of the ferrocene-containing complex **2** and model complex **1**.

2. Experimental Section

2.1. Materials

All reagents and chemicals were purchased from commercial sources and used without further purification. The solvents were purified by routine procedures and distilled under dry N_2 . Ferroceneboronic acid was purchased from Pharmaceutical Group Co., Ltd. (Shanghai, China). All other ligands and materials were purchased from either Aldrich Co., Ltd. (Shanghai, China) or Pharmaceutical Group Co., Ltd. (Shanghai, China).

2.2. Characterization and Methods

1H NMR (400 MHz) was recorded by a Bruker Ultra Shield Plus 400 MHz NMR instruments. Mass spectrum (MS) was obtained on a Bruker autoflex MALDI-TOF/TOF mass spectrometer. The UV-visible absorption spectrum was measured with Shimadzu UV-3600 Spectrophotometer. Scanning electron microscope (SEM) images were measured using Hitachi S4800 scanning electron microscope. Atomic force microscope (AFM) images were measured using Dimension Icon atomic force microscope. Cyclic voltammetry (CV) was performed with an Autolab CHI 660E electrochemical analyzer using glassy carbon electrode as working electrode and platinum wire as an auxiliary electrode and ferrocene as standard at a scan rate of 50 mV/s against an Ag/AgCl reference electrode in acetonitrile (CH_3CN) solution of 0.1 M Bu_4NPF_6 under a nitrogen atmosphere. The complex was coated on Pt plate electrode by dipping the electrode into the corresponding solution and then

drying. The I-V characteristics of the devices were measured by the Keithley 2636A semiconductor parameter analyzer. The two probes of the semiconductor parameter analyzer are connected to the two electrodes (ITO and Al) of the device respectively, and the measured voltage and current values are fed back to the programmed computer program where the voltage range is set to -5 V to +5 V. As the voltage increases, the I-V curve of the device is measured, and the memory type of the device is determined according to the I-V curve. All theoretical calculations were carried out with the Gaussian 09 package. Density functional theory (DFT) was utilized to model and optimize the molecular structure at the B3LYP/LanL2DZ level. In particular, the HOMO and LUMO level positions and related electron cloud distributions were calculated with isovalue = 0.04.

2.3. Synthesis

2.3.1. Synthesis of M1

4-Bromophenylboronic acid (0.63 g, 3.15 mmol), 2-bromopyridine (0.79 g, 5.00 mmol) and Pd(PPh₃)₄ (0.05 g) were added to the mixture of ethanol (5 mL), toluene (15 mL) and saturated Na₂CO₃ (5 mL). The mixture was stirred at 85 °C for 7 h under N₂. After the reaction was completed, the mixture was diluted with dichloromethane, dried over anhydrous Na₂CO₃, and then the solvent was evaporated. The crude product was purified by column chromatography on silica using ethyl acetate: petroleum ether (1/1, v/v) to give **M1** as white flake crystal. ¹H NMR (400 MHz, DMSO-d₆, δ): 8.65 (ddd, *J* = 4.7, 1.7, 0.8 Hz, 1H), 8.07–8.00 (m, 2H), 7.97 (d, *J* = 8.0 Hz, 1H), 7.88 (td, *J* = 7.7, 1.7 Hz, 1H), 7.67 (dd, *J* = 8.9, 2.1 Hz, 2H), 7.37 (ddd, *J* = 7.4, 4.8, 0.9 Hz, 1H).

2.3.2. Synthesis of M2

M1 (116.50 mg, 0.50 mmol), Pd(PPh₃)₄ (15.00 mg) and K₃PO₄ (212.00 mg) were added to a solution of ferroceneboronic acid (138.00 mg, 0.60 mmol) in 1,4-dioxane (20 ml). The mixture was stirred at 100 °C for 24 h under N₂. After the reaction was completed, the solvent was removed under reduced pressure. The crude product was purified by column chromatography on silica using ethyl acetate: petroleum ether to give **M2** as yellow brown solid with the yield of 52%. ¹H NMR (400 MHz, CDCl₃, δ):

8.70 (dt, $J = 4.8, 1.4$ Hz, 1H), 7.95–7.91 (m, 2H), 7.77–7.72 (m, 2H), 7.61–7.56 (m, 2H), 7.25–7.19 (m, 1H), 4.74–4.69 (m, 2H), 4.38–4.34 (m, 2H), 4.06 (s, 5H).

2.3.3. Synthesis of M3

To the mixture of $\text{IrCl}_3 \cdot 3\text{H}_2\text{O}$ (64.40 mg, 0.18 mmol) and **M2** (130.00 mg, 0.38 mmol), 2-ethoxyethanol (6 mL) and H_2O (2 mL) were added. The mixture was stirred at 110 °C for 24 h under N_2 . After the mixture was cooled to room temperature, the resulting powder was filtered and washed with ethanol. The obtained solid **M3** was dried under vacuum and used next step directly.

2.3.4. Synthesis of complex 2

To the mixture of **M3** (226.00 mg, 0.13 mmol), pentane-2,4-dione (40.00 mg, 0.40 mmol) and K_2CO_3 (50.00 mg), CH_2Cl_2 (20 mL) was added. The mixture was stirred at 25 °C for 24 h under N_2 . After the reaction, the crude product was purified by column chromatography on silica using acetone: petroleum ether (1/1, v/v) to give complex **2** as red brown solid with the yield of 68%. ^1H NMR (400 MHz, CDCl_3 , δ): 8.60 (d, $J = 5.1$ Hz, 2H), 7.90 (d, $J = 8.0$ Hz, 2H), 7.87–7.79 (m, 2H), 7.41 (d, $J = 8.1$ Hz, 2H), 7.21 (ddd, $J = 7.3, 5.9, 1.3$ Hz, 2H), 6.79 (dd, $J = 8.1, 1.7$ Hz, 2H), 6.41 (d, $J = 1.5$ Hz, 2H), 5.30 (s, 1H), 4.33 (s, 2H), 4.29–4.23 (m, 2H), 4.12 (dd, $J = 3.6, 1.5$ Hz, 4H), 3.71 (s, 10H), 1.88–1.82 (s, 6H). MALDI-TOF-MS (m/z): calcd for $\text{C}_{47}\text{H}_{39}\text{Fe}_2\text{IrN}_2\text{O}_2$, 968.13; found, 968.15.

2.4. Fabrication of Memory Devices

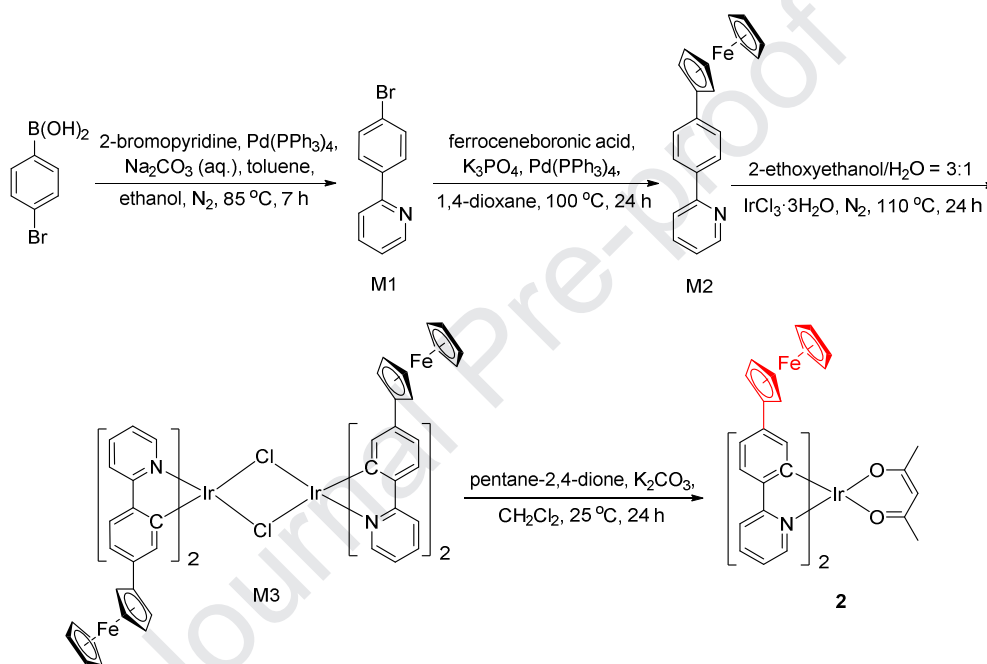
The memory devices **D1** and **D2** were fabricated based on ITO/ complex **1** or **2**/Al sandwiched structure, respectively. The ITO glass substrate was pre-cleaned with deionized water, acetone, and then isopropanol in an ultrasonic bath (15 min). The active layer (complex **1** or **2**) was deposited under high vacuum (about 10^{-5} Pa). The film thickness was about 80 nm. An Al layer with a thickness of about 100 nm was thermally evaporated and deposited onto the organic surface at about 10^{-5} Pa through a shadow mask to form the top electrode.

3. Results and Discussion

3.1. Synthesis

The synthetic routes of complex **2** are outlined in **Scheme 1**. For complex **2**, there are

two main steps: (1) Ferrocene-containing ligand was firstly prepared by Suzuki coupling reaction. (2) Under N_2 , **M3** (226.00 mg, 0.13 mmol), pentane-2,4-dione (40.00 mg, 0.40 mmol) and K_2CO_3 (50.00 mg) were dissolved in a solution of CH_2Cl_2 (20 mL). The mixture was stirred for 24 h at 25 °C. The residue was purified by column chromatography on silica using acetone and petroleum ether to give the red brown solid. The synthesis of complex **1** is based on the report of literature.⁴² Their chemical structures were characterized by 1H NMR and MS (**Figure S1, S2, S3 and S4**).



Scheme 1. The synthetic routes of ferrocene-containing complex **2**.

3.2. Photophysical Property

The optical properties of complex **1** and **2** were investigated in THF at 298 K. As shown in **Figure 2A**, the UV-visible absorption spectrum of complex **2** showed similar features with that of complex **1**. According to the literature,^{42,43} the absorption peak at about 350 nm was attributed to the singlet π - π^* transition of ppy ligand. The absorption peak at about 500 nm was attributed to the singlet and triplet metal-to-ligand charge transfer transition (MLCT). Compared with complex **1**, the introduction of ferrocene has little effect on the absorption spectra. With the presence of ferrocene groups on the ligands, complex **2** showed non-luminescence due to the ferrocene quenching emission (**Figure S5**).^{44, 45}

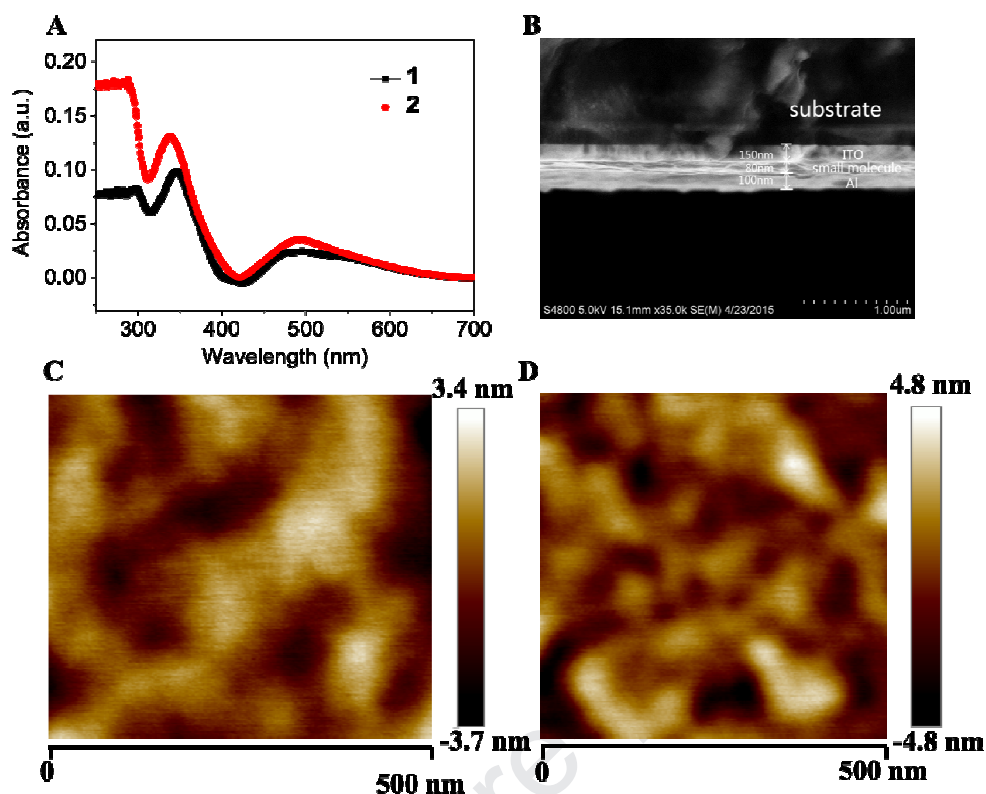


Figure 2. (A) UV-visible absorption spectra of complex **1** and **2** in THF solutions (1.0×10^{-5} mol/L); (B) SEM image of **D2**; (C) AFM image of **D1**; (D) AFM image of **D2**.

3.3. Morphologies of the film and devices

The morphology was also examined by SEM images. The layer thicknesses of top Al electrode, complex **2** film and bottom ITO electrode were determined to be about 100 nm, 80 nm and 150 nm, respectively (**Figure 2B**). AFM images in **Figure 2C** and **2D** showed that the root-mean-square roughness of the film for complex **1** and **2** was ca. 0.74 and 1.18 nm, respectively. The remarkable smoothness is considered to be the weak π - π stacking in the film, and the smooth interface is considered to be favorable for charge transport, resulting in low threshold voltage.

3.4. Characterization of memory device

The memory behaviors of complex **2** have been investigated by current-voltage (I-V) measurements of the device **D2** (**Figure 3B**). Initially, **D2** was in a low conduction state. A suddenly sharp increase in the current was observed at the threshold voltage of -0.55 V (the first sweep), which indicated that **D2** switched from OFF state ($\sim 10^{-5}$ A, “0” state) to ON state ($\sim 10^{-2}$ A, “1” state). The ON/OFF current ratio was as high as

10^3 , which is sufficient to function with a low misreading error. The switch is considered as the “writing” process. In the second sweep from -4 to 0 V, the ON state can be maintained, which indicated that **D2** demonstrated excellent stability. **D2** can be retained even after the power is removed, suggesting that the memory effect is non-volatile.³⁵ This transition is equivalent to the “read” process. **D2** switches from ON to OFF state after applying a reverse voltage of 2.68 V (the third sweep), and this transition is considered as “erase” process. The OFF state can be maintained during the fourth sweep. Thus, the “write–read–erase–read” cycle was accomplished and **D2** shared similar characteristics with flash memory. For the repeat sweep 5-8, the I–V characteristics of **D2** exhibit the same behavior. However, **D1** without ferrocene groups does not exhibit a bistability or memory effect (**Figure 3A**). Thus, ferrocene groups play a key role in the switching behavior of complex **2**.

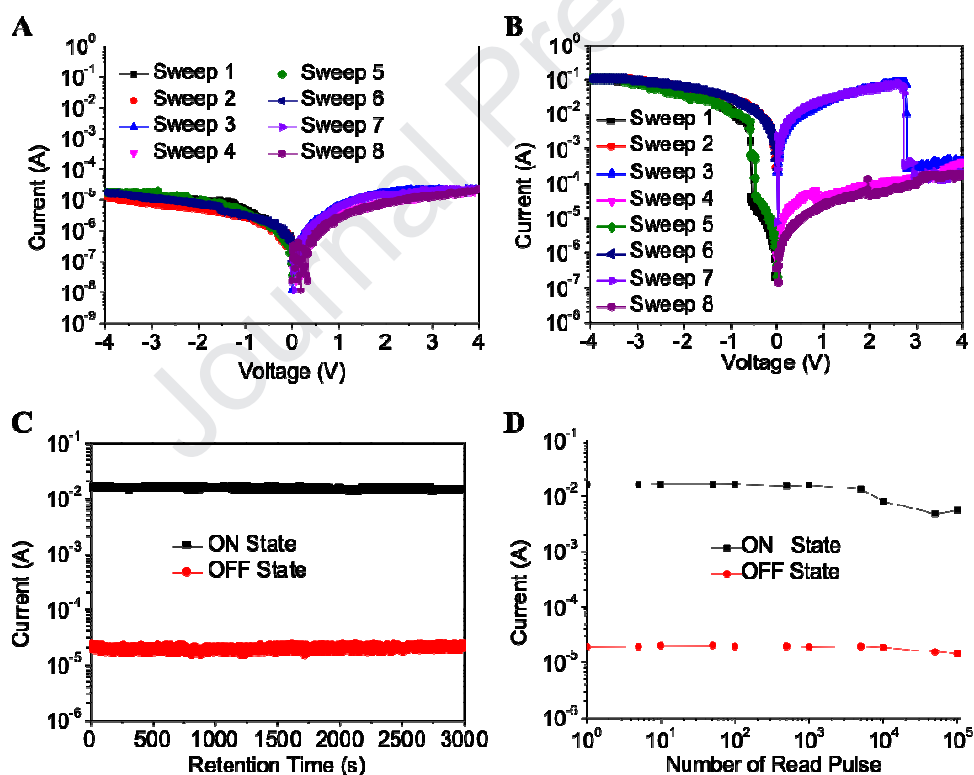


Figure 3. (A) I–V characteristic curve of **D1**; (B) I–V characteristic curve of **D2**; (C) Retention time of **D2**; (D) Number of read pulses of **D2**.

We have summarized the flash memory performance of devices containing metal complexes in recent years. The comparison of memory performance with other related works was shown in **Table S1** (Molecular structures were shown in **Figure S6**).⁴⁶⁻⁵⁴

The memory based on complex **2** showed the minimum threshold voltage. Low power consumption memory requires low operating voltage. **D2** shows good stability and durability comparing with other devices containing metal complexes. **D2** remains stable for at least 10^3 s at a continuous stress of 1.0 V for both ON and OFF states (**Figure 3C**). No obvious degradation was observed after more than 10^5 read cycles for both the ON and OFF states at a read voltage of 1.0 V (**Figure 3D**). This result demonstrates that **D2** exhibits an excellent retention and stability of both states.^{55,56}

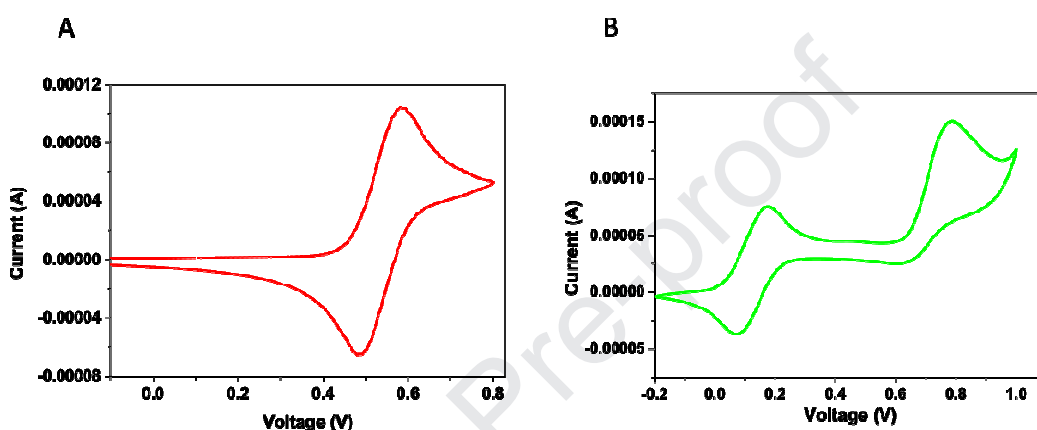


Figure 4. CV of complex **1** (A) and **2** (B) in acetonitrile.

In order to understand the memory mechanism of **D2**, the redox characteristics of the complexes were performed by CV with ferrocene as standard in acetonitrile (CH_3CN) solution of 0.1 M Bu_4NPF_6 under nitrogen atmosphere (**Figure 4**). The HOMO and LUMO energy levels of complex **2** can be calculated to be -4.86 eV and -2.88 eV, respectively, by the equations $E_{\text{HOMO}} = -(E_{1/2}^{\text{Ox1}} + 4.8 - E_{\text{Ferrocene}})$, $E_g = hc/\lambda_{\text{Edge}}$, $E_{\text{LUMO}} = E_{\text{HOMO}} + E_g$. Similarly, the HOMO and LUMO energy levels of complex **1** are -5.26 and -3.35 eV, respectively (**Table 1**).

Table 1. Photophysical and electrochemical properties of complex **1** and **2**

Complex	$\lambda_{\text{max}} / \text{nm}$	$\lambda_{\text{Edge}} / \text{nm}$	$E_{1/2}^{\text{Ox1}} / \text{eV}$	E_g / eV	HOMO / eV	LUMO / eV
1	300, 347, 491	649	0.55	1.91	-5.26	-3.35
2	287, 338, 491	627	0.15	1.98	-4.86	-2.88

It can be seen from **Figure 5**, the energy barrier (E) between the HOMO level of complex **2** and the work function (W) of ITO (-4.8 eV) is 0.06 eV, which is much smaller than that of complex **1** (0.46 eV). Similarly, the E between the LUMO level of

complex **2** and the W of Al (-4.3 eV) is 1.42 eV and that of complex **1** is 0.95 eV. These results indicated that the hole injection of complex **2** is a more favorable process and hole transportation dominates the conducting process.^{44, 47}

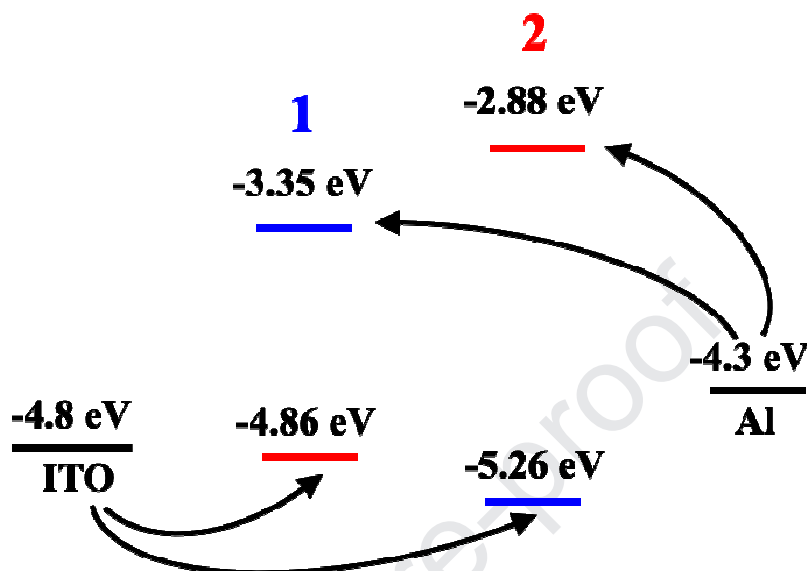


Figure 5. Schematic diagram of the charge transition process in **D1** or **D2**.

The HOMO and LUMO energy levels of the complex **2** were investigated by density functional theory (DFT) calculations (**Figure 6**). The calculated HOMO of complex **2** is located on the ferrocene group. When a negative bias is applied for the first sweep from 0 to -4 V, Fe^{2+} could be oxidized to Fe^{3+} . As a result, **D2** can be easily changed from the OFF state to the ON state *via* the oxidation of ferrocene units ($\text{Fe}^{2+} - e \rightarrow \text{Fe}^{3+}$) and charge transferred from ferrocene to iridium(III) complex, resulting in a low threshold voltage at -0.55 V. **D2** changes more conducting when electrons were gained/lost during the redox process and hold the memory on the ON state, resulting in the non-volatile flash performance. Due to the steric hindrance of iridium(III), **D2** exhibits higher OFF switch voltage of 2.68 V when a reverse voltage is applied. This natural performance of ferrocene evidently underlies the non-volatile flash memory device applications of the manufactured ferrocene-containing complexes.^{34-36, 45}

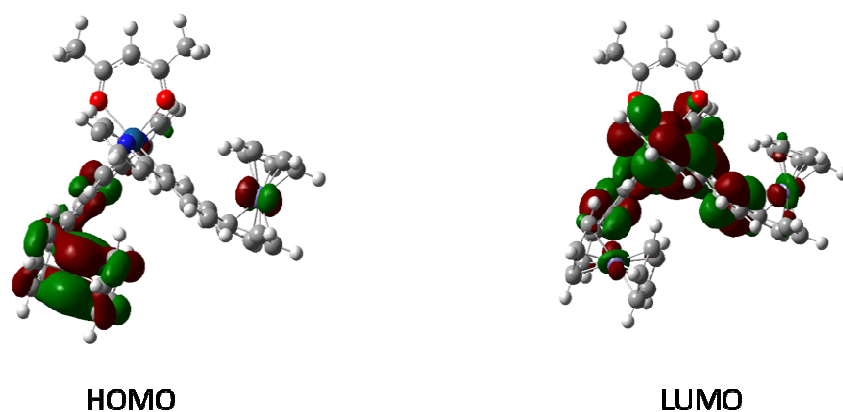


Figure 6. Calculated HOMO and LUMO of complex **2**.

4. Conclusion

In summary, a new ferrocene-containing iridium(III) complex has been synthesized and applied in flash memory device. The memory device of ITO/complex **2**/Al exhibits flash memory characters with a high ON/OFF current ratio of 10^3 , long retention time of 10^3 s, low threshold voltage of -0.55 V, and large read cycles up to 10^5 . Based on the in-depth analysis of I–V, CV and DFT data, a redox memory mechanism is proposed to explain the conductive process. This work proves that the ferrocene-containing iridium(III) complexes show great potential applications in future small molecular non-volatile memory devices.

5. Acknowledgments

We acknowledge financial support from the National Funds for Distinguished Young Scientists (61825503), National Natural Science Foundation of China (51473078, 21671108 and 61905120), Natural Science Foundation of Jiangsu Province of China (BK20190740), Priority Academic Program Development of Jiangsu Higher Education Institutions (YX03001), China Postdoctoral Science Foundation Funded Project (2018M640506), Jiangsu Planned Projects for Postdoctoral Research Funds (2018K003B), the Scientific Foundation of Nanjing University of Posts and Telecommunications (NUPTSF) (NY218123).

6. References

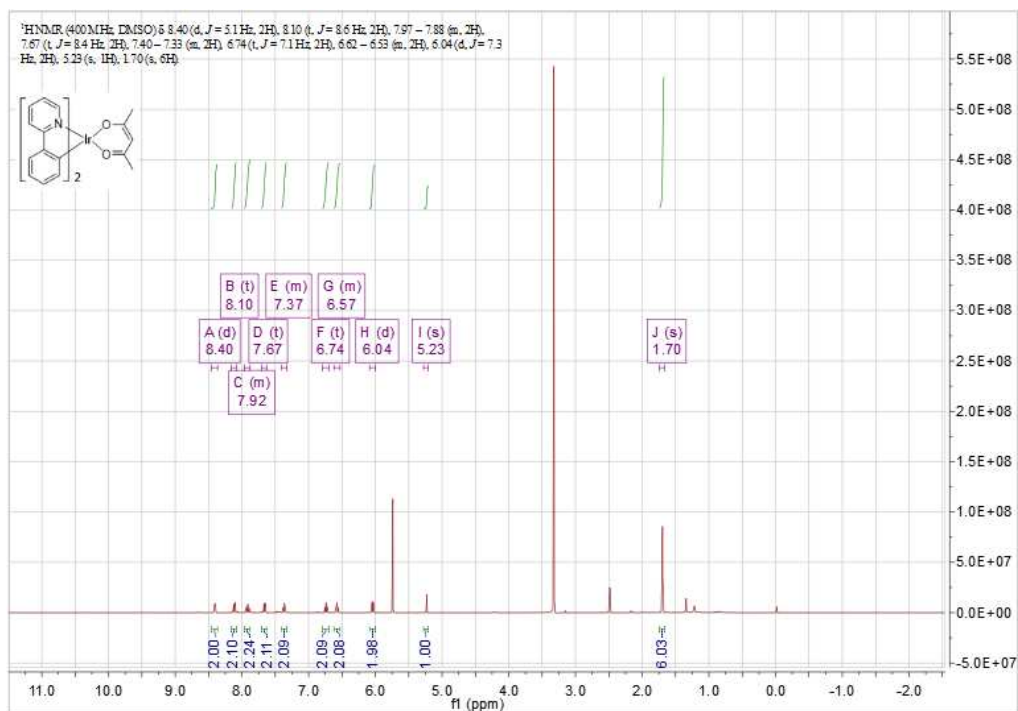
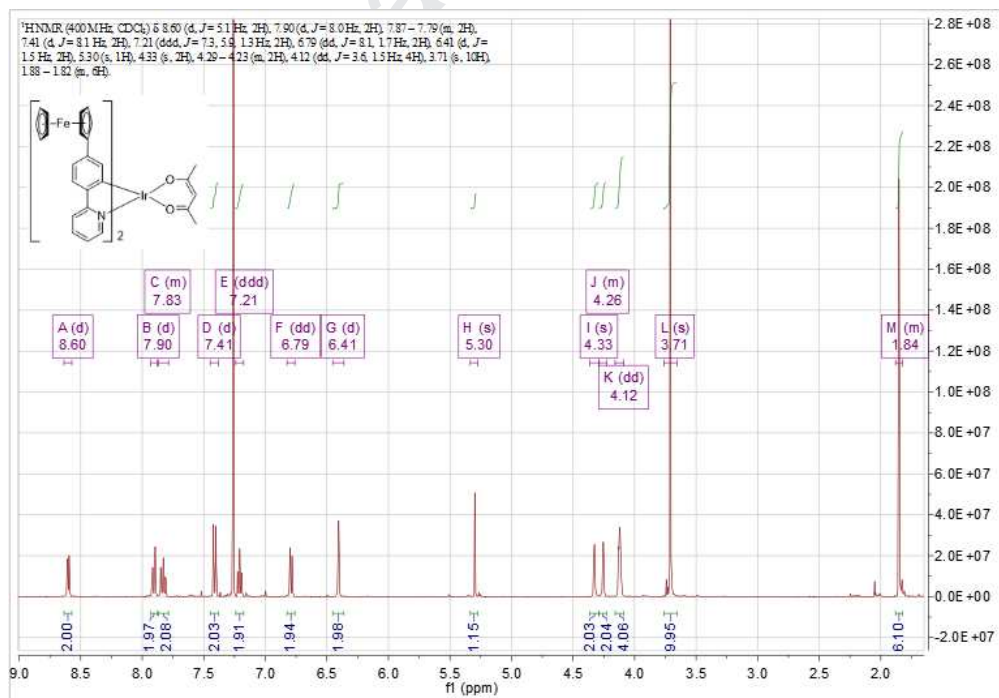
- 1 B. Zhang, L. Liu, L. Wang, B. Liu, X. Tian and Y. Chen, *Carbon*, 2018, **134**, 500-506.
- 2 H. Wang, F. Zhou, L. Wu, X. Xiao, P. Y. Gu, J. Jiang, Q. F. Xu and J. M. Lu, *Polym. Chem.*, 2018, **9**, 1139-1146.
- 3 P. Dagar, J. Bera, G. Vyas and S. Sahu, *Org. Electron.*, 2019, **71**, 303-311.
- 4 H. Li, H. Li, Q. Zhang and J. Lu, *Org. Electron.*, 2019, **73**, 255-260.
- 5 M. Xu, S. Guo, T. Xu, W. Xie and W. Wang, *Org. Electron.*, 2019, **64**, 62-70.
- 6 Y. Xin, X. Zhao, H. Zhang, S. Wang, C. Wang, D. Ma and P. Yan, *Org. Electron.*, 2019, **74**, 110-117.
- 7 K. Zhang, X. Feng, C. Ye, M. A. Hempenius and G. J. Vancso, *J. Am. Chem. Soc.*, 2017, **139**, 10029-10035.
- 8 Y. Yang, J. Ouyang, L. Ma, R. J. H. Tseng and C. W. Chu, *Adv. Funct. Mater.*, 2006, **16**, 1001-1014.
- 9 X. Yang, G. Zhou and W. Y. Wong, *Chem. Soc. Rev.*, 2015, **44**, 8484-8575.
- 10 W. Ruan, Y. Hu, F. Xu and S. Zhang, *Org. Electron.*, 2019, **70**, 252-257.
- 11 C. Su, Y. Ye, L. Xu and C. Zhang, *J. Mater. Chem.*, 2012, **22**, 22658-22662.
- 12 J. C. Scott and L. D. Bozano, *Adv. Mater.*, 2007, **19**, 1452-1463.
- 13 J. C. Scott, *Science*, 2004, **304**, 62-63.
- 14 R. Pietschnig, *Chem. Soc. Rev.*, 2016, **45**, 5216-5231.
- 15 J. Y. Ouyang, C. W. Chu, C. R. Szmada, L. P. Ma and Y. Yang, *Nat. Mater.*, 2004, **3**, 918-922.
- 16 P. Wang, S. J. Liu, Z. H. Lin, X. C. Dong, Q. Zhao, W. P. Lin, M. D. Yi, S. H. Ye, C. X. Zhu and W. Huang, *J. Mater. Chem.*, 2012, **22**, 9576-9583.
- 17 D. R. van Staveren and N. Metzler-Nolte, *Chem. Rev.*, 2004, **104**, 5931-5985.
- 18 R. J. Tseng, J. X. Huang, J. Ouyang, R. B. Kaner and Y. Yang, *Nano Lett.*, 2005, **5**, 1077-1080.
- 19 R. Tong, Y. Zhao, L. Wang, H. Yu, F. Ren, M. Saleem and W. A. Amer, *J. Organomet. Chem.*, 2014, **755**, 16-32.
- 20 C. D. Muller, A. Falcou, N. Reckefuss, M. Rojahn, V. Wiederhirn, P. Rudati, H.

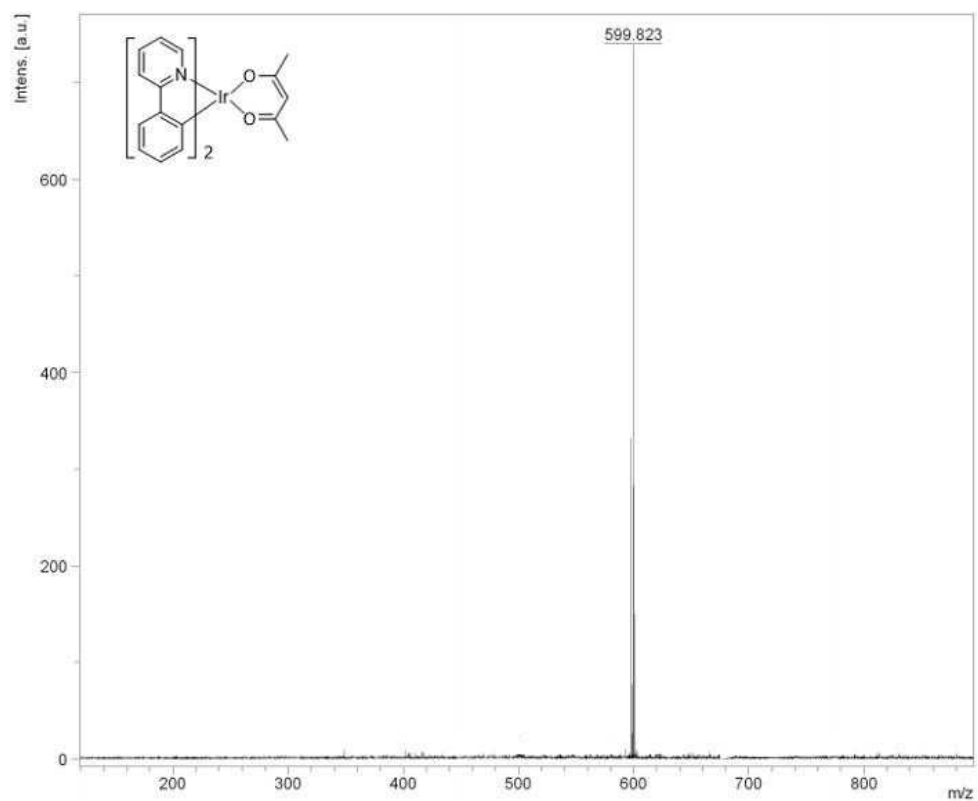
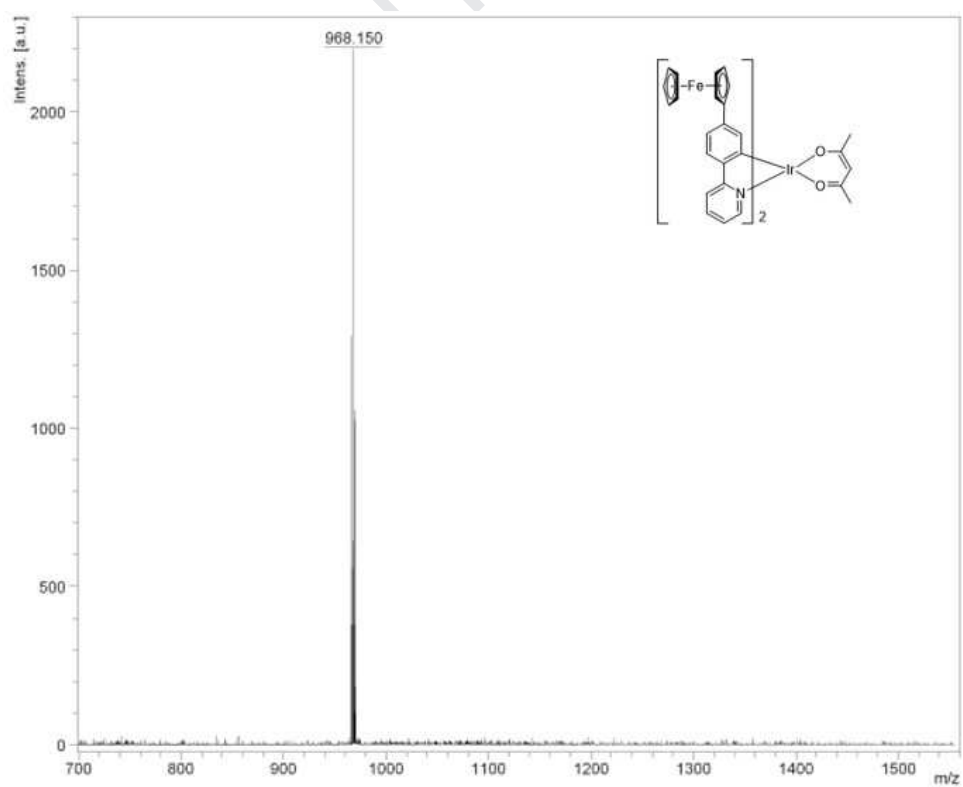
- Frohne, O. Nuyken, H. Becker and K. Meerholz, *Nature*, 2003, **421**, 829-833.
- 21 T. Morikita and T. Yamamoto, *J. Organomet. Chem.*, 2001, **637**, 809-812.
- 22 C. Moorlag, B. C. Sih, T. L. Stott and M. O. Wolf, *J. Mater. Chem.*, 2005, **15**, 2433-2436.
- 23 S. Moller, C. Perlov, W. Jackson, C. Taussig and S. R. Forrest, *Nature*, 2003, **426**, 166-169.
- 24 Y. L. Liu, K. L. Wang, G. S. Huang, C. X. Zhu, E. S. Tok, K. G. Neoh and E. T. Kang, *Chem. Mater.*, 2009, **21**, 3391-3399.
- 25 S. J. Liu, P. Wang, Q. Zhao, H. Y. Yang, J. Wong, H. B. Sun, X. C. Dong, W. P. Lin and W. Huang, *Adv. Mater.*, 2012, **24**, 2901-2905.
- 26 S. J. Liu, Z. H. Lin, Q. Zhao, Y. Ma, H. F. Shi, M. D. Yi, Q. D. Ling, Q. L. Fan, C. X. Zhu, E. T. Kang and W. Huang, *Adv. Funct. Mater.*, 2011, **21**, 979-985.
- 27 S. J. Liu, W. P. Lin, M. D. Yi, W. J. Xu, C. Tang, Q. Zhao, S. H. Ye, X. M. Liu and W. Huang, *J. Mater. Chem.*, 2012, **22**, 22964-22970.
- 28 F. Fan, B. Zhang, S. Song, B. Liu, Y. Cao and Y. Chen, *Adv. Electron. Mater.*, 2018, **4**, 1700397.
- 29 Q. D. Ling, Y. Song, S. L. Lim, E. Y. H. Teo, Y. P. Tan, C. Zhu, D. S. H. Chan, D. L. Kwong, E. T. Kang and K. G. Neoh, *Angew. Chem. Int. Ed.*, 2006, **45**, 2947-2951.
- 30 Q. D. Ling, F. C. Chang, Y. Song, C. X. Zhu, D. J. Liaw, D. S. H. Chan, E. T. Kang and K. G. Neoh, *J. Am. Chem. Soc.*, 2006, **128**, 8732-8733.
- 31 W. P. Lin, S. J. Liu, T. Gong, Q. Zhao and W. Huang, *Adv. Mater.*, 2014, **26**, 570-606.
- 32 E. Y. Hong, C. T. Poon and V. W. Yam, *J. Am. Chem. Soc.*, 2016, **138**, 6368-6371.
- 33 V. K. M. Au, D. Wu and V. W. W. Yam, *J. Am. Chem. Soc.*, 2015, **137**, 4654-4657.
- 34 T. L. Choi, K. H. Lee, W. J. Joo, S. Lee, T. W. Lee and M. Y. Chae, *J. Am. Chem. Soc.*, 2007, **129**, 9842-9843.
- 35 C. Jin, J. Lee, E. Lee, E. Hwang and H. Lee, *Chem. Commun.*, 2012, **48**, 4235-4237.
- 36 C. K. Kim, W.-J. Joo, E. S. Song, H. J. Kim, J. Kim, C. Park, H. L. Lee and C.

- Kim, *Synth. Met.*, 2007, **157**, 640-643.
- 37 B. Zhang, F. Fan, W. Xue, G. Liu, Y. Fu, X. Zhuang, X. H. Xu, J. Gu, R. W. Li and Y. Chen, *Nat. Commun.*, 2019, **10**, 736.
- 38 H. Tan, H. Yao, Y. Song, S. Zhu, H. Yu and S. Guan, *Dyes. Pigments.*, 2017, **146**, 210-218.
- 39 B. B. Cui, J. H. Tang and Y. W. Zhong, *Acta Chim. Sinica*, 2016, **74**, 726-733.
- 40 W. P. Lin, S. J. Liu, T. Gong, Q. Zhao and W. Huang, *Adv. Mater.*, 2014, **26**, 570-606.
- 41 Q. D. Ling, D. J. Liaw, C. Zhu, D. S. H. Chan, E. T. Kang and K. G. Neoh, *Prog. Polym. Sci.*, 2008, **33**, 917-978.
- 42 S. Lamansky, P. Djurovich, D. Murphy, F. Abdel-Razzaq, R. Kwong, I. Tsyba, M. Bortz, B. Mui, R. Bau and M. E. Thompson, *Inorg. Chem.*, 2001, **40**, 1704-1711.
- 43 Z. Ye, J. Yang, Z. Ling, Y. Zhao, G. Chen, Y. Zheng, B. Wei and Y. Shi, *Chin. J. Org. Chem.*, 2019, **39**, 449-455.
- 44 J. Xiang, X. L. Li, Y. Ma, Q. Zhao, C. L. Ho and W. Y. Wong, *J. Mater. Chem. C*, 2018, **6**, 11348-11355.
- 45 J. Xiang, T. K. Wang, Q. Zhao, W. Huang, C. L. Ho and W. Y. Wong, *J. Mater. Chem. C*, 2016, **4**, 921-928.
- 46 J. H. Tang, T. G. Sun, J. Y. Shao, Z. L. Gong and Y. W. Zhong, *Chem. Commun.*, 2017, **53**, 11925-11928.
- 47 R. Hao, N. Jia, G. Tian, S. Qi, L. Shi, X. Wang and D. Wu, *Mater. Des.*, 2018, **139**, 298-303.
- 48 S. J. Liu, Z. H. Lin, Q. Zhao, Y. Ma, H. F. Shi, M. D. Yi, Q. D. Ling, Q. L. Fan, C. X. Zhu, E. T. Kang and W. Huang, *Adv. Funct. Mater.*, 2011, **21**, 979-985.
- 49 S. J. Liu, W. P. Lin, M. D. Yi, W. J. Xu, C. Tang, Q. Zhao, S. H. Ye, X. M. Liu and W. Huang, *J. Mater. Chem.*, 2012, **22**, 22964-22970.
- 50 W. Lin, H. Sun, S. Liu, H. Yang, S. Ye, W. Xu, Q. Zhao, X. Liu and W. Huang, *Macromol. Chem. Phys.*, 2012, **213**, 2472-2478.
- 51 P. Wang, S. J. Liu, Z. H. Lin, X. C. Dong, Q. Zhao, W. P. Lin, M. D. Yi, S. H. Ye, C. X. Zhu and W. Huang, *J. Mater. Chem.*, 2012, **22**, 9576.

- 52 N. D. Paul, U. Rana, S. Goswami, T. K. Mondal and S. Goswami, *J. Am. Chem. Soc.*, 2012, **134**, 6520-6523.
- 53 B.-B. Cui, Z. Mao, Y. Chen, Y.-W. Zhong, G. Yu, C. Zhan and J. Yao, *Chem. Sci.*, 2015, **6**, 1308-1315.
- 54 S. Goswami, A. J. Matula, S. P. Rath, S. Hedstrom, S. Saha, M. Annamalai, D. Sengupta, A. Patra, S. Ghosh, H. Jani, S. Sarkar, M. R. Motapothula, C. A. Nijhuis, J. Martin, S. Goswami, V. S. Batista and T. Venkatesan, *Nat. Mater.*, 2017, **16**, 1216-1224.
- 55 S. Goswami, D. Sengupta, N. D. Paul, T. K. Mondal and S. Goswami, *Chemistry*, 2014, **20**, 6103-6111.
- 56 S. J. Liu, P. Wang, Q. Zhao, H. Y. Yang, J. Wong, H. B. Sun, X. C. Dong, W. P. Lin and W. Huang, *Adv. Mater.*, 2012, **24**, 2901-2905.

Supporting Information

Figure S1. The enlarged view of ¹H NMR spectra of complex 1Figure S2. The enlarged view of ¹H NMR spectra of complex 2

**Figure S3.** MS of complex 1**Figure S4.** MS of complex 2

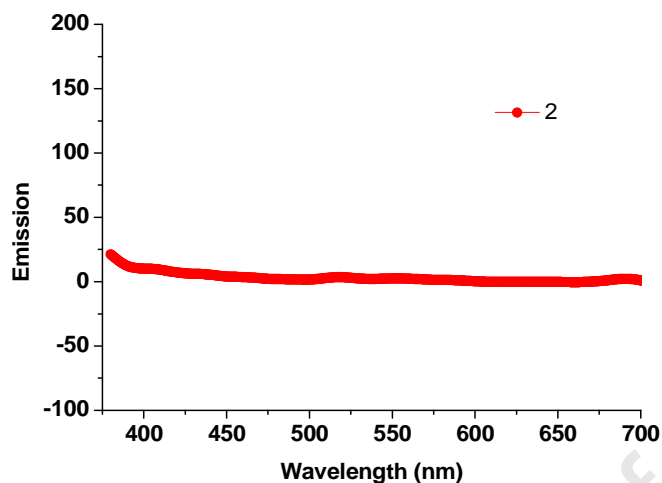


Figure S5. Photoluminescence spectra of complex **2**

Table S1. Comparing the flash memory performance with other related works

Complex	“writing” voltage/V	ON/OFF current ratio	“erase” voltage/V	retention time/s	read cycles
2	-0.55	10^3	2.68	10^3	10^5
a ⁴⁶	-0.6	$>10^3$	2.6	$>10^3$	$>10^3$
b ⁴⁷	1.4	10^3	-3.2	10^3	10^8
c ⁴⁸	-1.6	10^5	2.8	10^3	10^8
d ⁴⁹	-1.2	10^3	4.1	10^4	$>10^7$
e ⁵⁰	-2.6	$>10^3$	3	10^3	$>10^7$
f ⁵¹	-1.5	10^3	4.1	10^3	10^7
g ⁵²	2.75	10^3	-2.05	10^2	$>10^2$
h ⁵³	3.4	10^2 - 10^3	-4.3	10^3	$>10^2$
i ⁵⁴	3.95 ± 0.21	10^4	-4.14 ± 0.19	$>10^6$	10^{12}

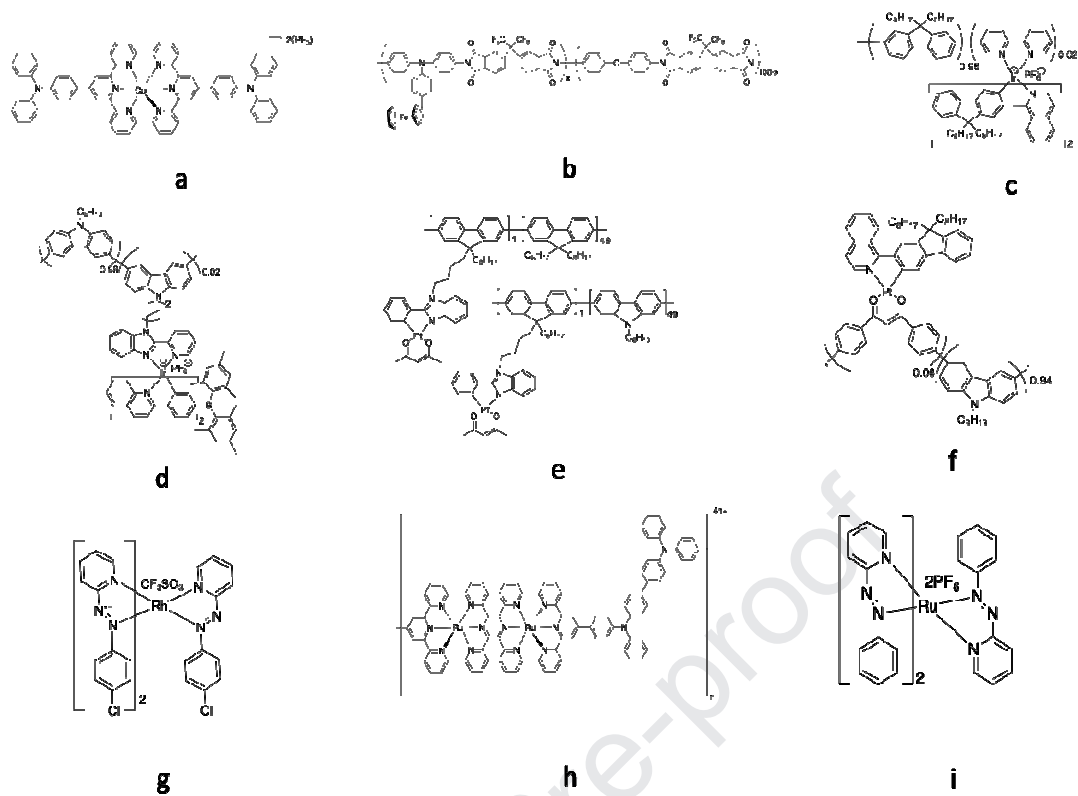


Figure S6. Molecular structures of **Table S1**

Highlights

- A new ferrocene-containing iridium(III) complex has been designed and synthesized.
- Ferrocene-containing iridium(III) complex exhibited non-volatile flash memory behavior with a low threshold voltage at -0.55 V.
- A redox mechanism was proposed to explain the conduction process. The transition from OFF state to ON state was induced by the redox of ferrocene units ($\text{Fe}^{2+} - \text{e}^- \rightarrow \text{Fe}^{3+}$).
- This work provides a new strategy to realize non-volatile flash memory devices by the employment of iridium(III) complexes with redox-active groups.

Declaration of interests

The authors declare that they have no known competing financial interests or personal relationships that could have appeared to influence the work reported in this paper.

The authors declare the following financial interests/personal relationships which may be considered as potential competing interests:

Journal Pre-proof